



Print ISSN: 0375-9237  
Online ISSN: 2357-0350

# EGYPTIAN JOURNAL OF BOTANY (EJBO)

Chairperson

**PROF. DR. MOHAMED I. ALI**

Editor-in-Chief

**PROF. DR. SALAMA A. OUF**

**Biogenic synthesis, characterization,  
optimization and antibacterial activities of  
silver nanoparticles (AgNPs) from  
*Aspergillus fumigatus* Eu.co against bacterial  
pathogens**

Doaa M. A. Khalil, Noura Sh. A. Hagaggi



PUBLISHED BY  
THE EGYPTIAN  
BOTANICAL SOCIETY

## Biogenic synthesis, characterization, optimization and antibacterial activities of silver nanoparticles (AgNPs) from *Aspergillus fumigatus* Eu.co against bacterial pathogens

Doaa M. A. Khalil<sup>1,2</sup>, Noura Sh. A. Hagaggi<sup>1</sup>

<sup>1</sup>Botany Department, Faculty of Science, Aswan University, Aswan, Egypt

<sup>2</sup>Unit of Environmental Studies and Development, Aswan University, Aswan, Egypt

The biogenic synthesis of silver nanoparticles (AgNPs) by using endophytic fungi is a potential biological nanomanufacturing technique that is cost-effective and environmentally friendly and represents a significant advancement for research in the field of nanotechnology. In this study, AgNO<sub>3</sub> was reduced to form silver nanoparticles (AgNPs) by using the mycelial filtrate of *Aspergillus fumigatus* Eu.co. The characteristics of the AgNPs were evaluated through UV-Visible Spectroscopy, X-Ray Diffraction (XRD), Scanning Electron Microscopy (SEM), Fourier Transform Infrared Spectroscopy (FTIR), and Elemental Diffraction X-Ray Spectroscopy (EDX) measurements. Furthermore, the applicability of AgNPs as antibacterial agents was detected against a numerous of pathogenic bacteria namely, *Salmonella typhi* (ATCC7251), *Escherichia coli* (ATCC 25922), *Enterobacter cloacae* (ATCC13047), and *Proteus mirabilis* (ATCC 29906) via a well diffusion assay. The biosynthesis of the biogenic AgNPs was shown by the color shift from yellow to dark brown. The highest UV absorption peak was detected at 420 nm. FTIR analysis of the AgNPs revealed the presence of alcohols, alkanes, unsaturated ketones, and aromatic, nitro and amide groups that are associated with bioactive compounds and serve as capping agents for the nanoparticles. XRD analysis of the AgNPs indicated a high degree of crystallinity. EDX spectrum showed a strong signal attributed to Ag nanocrystals. The optimum parameters of the AgNPs were the optimum temperature of 25°C, a neutral pH, 1.0 mM concentration of AgNO<sub>3</sub> and the reaction time of 144 hrs. AgNPs were more effective against *Enterobacter cloacae* ATCC13047, with an inhibition diameter of 59±1.01 mm.

**Keywords:** Nanotechnology, Biosynthesis, *Aspergillus fumigatus*, Antibacterial, Silver, Nanoparticles

### ARTICLE HISTORY

Submitted: April 06, 2025

Accepted: May 21, 2025

### CORRESPONDENCE TO

**Doaa M. A. Khalil**,  
Botany Department, Faculty of Sciences,  
Aswan University, Aswan, Egypt  
Email: doaa.khalil30@sci.aswu.edu.eg  
ORCID: orcid.org/0000-0002-9875-979X  
DOI: 10.21608/ejbo.2025.373896.3258

EDITED BY: S. Abd Ellatif

©2025 Egyptian Botanical Society

## INTRODUCTION

Nanobiotechnology has rapidly been considered as a major field in recent studies, with the most potential applications in medicine and agriculture. The biogenic or green approach for the biosynthesis of silver nanoparticles is a clean, efficient, and environmentally friendly method (Ahmad et al., 2024). Silver nanoparticles serve as a critical role in the fields of diagnostic procedures, therapeutic applications and drug delivery (Rai et al., 2021). Numerous advantages of nanoparticles in agriculture have been documented, including the application of nanopesticides, nanofertilizers, and plant growth stimulation (Paramo et al., 2020; El-Khouly et al., 2024; Soliman et al., 2024). Different nanoparticles can be produced via chemical, physical, and biological techniques. The biological methods used to produce these nanoparticles are low cost, reliable, and biodegradable (Ramos et al., 2020). Recently, AgNPs have garnered much interest due to their distinctive chemical and physical characteristics (Dhaka et al., 2023). AgNPs exhibit variations in chemical composition, size, shape and other characteristics (Al-Limoun et al., 2020).

Numerous uses of AgNPs in nanomedicine, such as microelectronics, catalysis, sensors, filters, antibacterial agents, and biolabeling, have been documented owing to their distinct physicochemical

and biological characteristics (Abbas et al., 2024). AgNPs have perfect antimicrobial capabilities that are durable in high-stress environments and useful for treating a variety of infectious agents (Huq et al., 2022). AgNPs are capable of being employed as alternative supervisory agents for the prevention of infectious agents together with various antifungal and antibacterial diseases because they exhibit low toxicity to humans at minimal concentrations (Huq & Akter, 2021). Moreover, AgNPs have good potential for use as anticancer agents (Dhaka et al., 2023).

Many microbes, such as fungi, bacteria, yeasts, and plants, are attracting much interest because of their capability to produce nanoparticles with high production yields and low costs (Huq, 2020). However, fungi are the most common method for creating AgNPs because they generate large amounts of protein, attain high yields, are easy to handle, are metal tolerant, and synthesize particles with low toxicity and capacity for bioaccumulation (Gezaf et al., 2022). Fungi are novel, environmentally sustainable and economical methods for producing nanoparticles and are considered excellent candidates due to their ability to synthesize high amounts of enzymes (Rai et al., 2021; Rami et al., 2024). Several scientific investigations have documented the successful production of AgNPs by

microbes, including fungi, yeasts, bacteria, actinomycetes, and microalgae (Fadiji et al., 2022). *Aspergillus falvus*, *Aspergillus niger*, *Aspergillus fumigatus*, *Aspergillus terreus*, *Aspergillus favipes*, *Penicillium oxalicum*, *Penicillium verrucosum*, *Fusarium scirpi*, *Cladosporium oxysporum*, *Alternaria carthami*, *Rhizopus stolonifer* and *Trichoderma harzianum* were recently investigated for their ability to synthesize AgNPs (Farrag et al., 2020; Rodríguez-Serrano et al., 2020; Lotfy et al., 2021; Yassin et al., 2021; Gupta et al., 2022; Khleifat et al., 2022a,b; Dadayya et al., 2023; Isaq et al., 2023; EL-Zawawy et al., 2023; Momenah et al., 2023; Moradi et al., 2024).

The current research aims to prepare and characterize AgNPs by utilizing the endophytic fungus *Aspergillus fumigatus* and to assess their antibacterial effectiveness against human infections.

## MATERIALS AND METHODS

### Microorganisms

The endophytic fungus *A. fumigatus* with accession number PQ876086 was previously isolated from *Eucalyptus camaldulensis* leaves. The culture was grown on potato dextrose agar plates, maintained at a temperature of 30°C and was stored at 4°C for preservation. *A. fumigatus* was obtained from the culture collection of the Mycology Laboratory, Faculty of Science, Aswan University, Egypt. The bacterial strains *Escherichia coli* (ATCC 25922), *Enterobacter cloacae* (ATCC13047), *Salmonella typhi* (ATCC7251), and *Proteus mirabilis* (ATCC 29906) were obtained from the culture collection of the Bacteriology Laboratory, Faculty of Science, Aswan University, Egypt.

### Biosynthesis of AgNPs

The culture and growth of the selected fungus *A. fumigatus* used for the biosynthesis of AgNPs were conducted following the modified protocols established by (Xue et al., 2016). In a 500 mL erlenmeyer flask with 200 mL of potato dextrose broth (PDB), the fungus was cultured and grew aerobically for 10 days at 28±2°C. The fungal biomass was harvested through filtration, then it was thoroughly cleaned numerous times using sterile distilled water. 10 grams (wet weight) of the fungal biomass was mixed with 100 milliliters of sterile distilled water, and the mixture was incubated at 28±2°C on an orbital shaker at 120 rpm. After 48 hrs., the mixture was filtered with Whatman filter paper No. 1. The mycelia filtrated was mixed with a silver nitrate (AgNO<sub>3</sub>) solution at a concentration of 1 mM at a volume/volume ratio of 1:1. The mixture was

incubated at 28°C for 24 hours in the dark to promote the production of AgNPs. Upon observing the color change to brown after an appropriate incubation time, the biosynthesized AgNPs were collected and purified through centrifugation at 15000 rpm for 15 minutes, which was repeated three times, with continuous washing using sterile distilled water to eliminate any residual substances.

### Optimization of Silver Nanoparticle Biosynthesis

Four primary factors were manipulated to optimize the AgNPs concentration: the concentration of silver nitrate, the temperature of the reaction, the duration, and the pH. These parameters were detected to increase the production of AgNPs. The biosynthesis of AgNPs was optimized by altering one parameter at a time. Various concentrations of AgNO<sub>3</sub> (1, 2, 3, 4, and 5 mM), temperatures (20, 30, 45, and 60°C), pH values (2, 3, 4, 7, and 9), and durations (24, 48, 72, 96, 120, and 144 hrs.) were detected. The absorbance of the resulting colored solution for each factor was measured at 420 nm via a UV-visible spectrophotometer. The optimal parameters were employed to synthesize AgNPs of superior grade. The procedure was described in earlier investigations carried out by (Abdel-Kareem et al., 2021).

### Characterization Techniques of AgNPs

The AgNPs formed during biosynthesis were examined via Ultraviolet-Visible Spectroscopy (UV-Vis), Scanning Electron Microscopy (SEM), Fourier Transform Infrared (FTIR) Spectroscopy, Energy Dispersive X-Ray (EDX) Spectroscopy, and X-Ray Diffraction (XRD) analysis.

### UV-Vis Spectroscopy Measurements

The color turning brown upon visual observation indicated the existence of AgNPs in the reaction media. The decrease of metal ions was verified by measuring the absorption using a T60U UV-Vis spectrophotometer (PG Instruments Ltd., China) in the 200–700 nm wavelength range. The absorbance was measured after 24 hrs. (Xue et al., 2016).

### Scanning Electron Microscopy (SEM)

SEM analysis was used to characterize the surface form of the biosynthesized AgNPs through SEM analysis (FE-SEM, QUANTA FEG 250, the Netherlands) (Janakiraman et al., 2019).

### Energy Dispersive X-Ray (EDX) Spectroscopy

The constituent element (Ag) of the biosynthesized AgNPs was analyzed via EDX spectroscopy, which was carried out at room temperature via a UV-1800

TOMOS spectrophotometer from China to detect the maximum wavelength ( $\lambda$  max.) of the AgNPs (Keshari et al., 2020).

#### Fourier Transform Infrared (FTIR) Spectroscopy

FTIR analysis was conducted using a JASCO 3600 (Tokyo, Japan), assisted by Agilent Technologies' Cary 630, to measure the spectral transmittance at room temperature. These spectral measurements covered a range from 400–4000  $\text{cm}^{-1}$  with a spectral resolution of 4  $\text{cm}^{-1}$ , aiming to identify and analyze the functional groups present in the formed AgNPs (Balakumaran et al., 2016).

#### X-Ray Diffraction (XRD) Analysis

The composition and structural properties of the purified AgNPs were examined via X-ray diffraction (XRD) on a Bruker AXS D8 instrument from Germany employing Cu K $\alpha$  radiation at a wavelength of 0.154 nm. Additionally, the peaks' location, width and strength were determined by analyzing the XRD pattern (Ali et al., 2023). The Debye-Scherrer equation was used to calculate the AgNPs' size (Dubey et al., 2010).

$$D = k \cdot \lambda / (\beta \cdot \cos \theta)$$

Where D is the average crystalline size of the nanoparticles, k is the geometric factor (0.9),  $\lambda$  is the wavelength of the X-ray radiation source ( $\lambda=1.5406 \text{ \AA}$ ) and  $\beta$  is the angular FWHM (full width at half maximum) of the XRD peak at the diffraction angle  $\theta$ .

#### Antibacterial Activities of the Synthesized AgNPs

The effectiveness of AgNPs was evaluated against four species of human pathogenic bacteria: *Salmonella typhi* (ATCC7251), *Escherichia coli* (ATCC 25922), *Enterobacter cloacae* (ATCC13047), and *Proteus mirabilis* (ATCC 29906), via the agar well diffusion technique. The tested bacteria were cultured in nutrient broth for 48 hrs. at a temperature of  $30^{\circ}\text{C} \pm 2^{\circ}\text{C}$ . Following this, under sterile conditions, the bacterial cultures were transferred onto Mueller–Hinton agar plates, where 6 mm wells were created. The AgNPs were prepared at a concentration of 1 mg/mL in 10% dimethyl sulfoxide (DMSO) as a negative control, and 50  $\mu\text{L}$  of this mixture was added to each well, whereas ampicillin at 1 mg/mL was used as a positive control. The diameters of the inhibition zones were recorded in millimeters after a 24 hrs. incubation period at  $37^{\circ}\text{C}$ . These experiments were conducted in triplicate (Baker et al., 2021).

#### Statistical Analysis

All experiments were conducted in triplicate. The statistical analysis was performed via Minitab 18 software (www.minitab.com). The data were subjected to one-way analysis of variance (ANOVA), and Tukey's post hoc test was used to evaluate statistical significance at a significance level of  $P < 0.05$ . The values shown in the figures are the means  $\pm$  standard errors (SEs).

### RESULTS

#### Biosynthesis of AgNPs

The AgNPs were successfully formed from an aqueous solution of  $\text{AgNO}_3$  by employing *A. fumigatus* mycelia filtrate and observe the change in color over time from light yellow to dark brown after 24 hrs. of incubation (Figure 1).

#### Optimization of AgNP Biosynthesis

The biosynthesis of AgNPs has been evaluated at different concentrations of  $\text{AgNO}_3$ . A 1.0 mM concentration was proved to be crucial for enabling the production of AgNPs (Figure 3a). As the  $\text{AgNO}_3$  concentration rose, the formed AgNPs' absorbance decreased. Therefore, a concentration of 1.0 mM was selected for the remaining tests in this investigation because of its higher absorbance than the other substrate concentrations.

The duration required for high production of AgNPs increased over a period ranging from 24–144 hrs. to detect the maximum period necessary for the reaction to achieve saturation. Figure 3b shows that a distinct peak emerged at 24 hrs., which continued to increase with increasing incubation time up to 144 hrs. The sixth day was determined to be the optimal incubation period for the biosynthesis of AgNPs. According to our findings, silver ion bioreduction exhibited optimal activity at an incubation temperature of  $30^{\circ}\text{C}$ , as shown in Figure 4a. This investigation revealed that the progress of AgNPs biosynthesis is enhanced by increasing the temperature to reach maximum at  $30^{\circ}\text{C}$  and then decreases when the temperature is increased to  $60^{\circ}\text{C}$ . In this investigation, we evaluated a pH range from 2–9 and reported that the most active range for AgNPs formation was between 6 and 7. No color change was detected at acidic pH values (2–4) in the AgNPs produced by *A. fumigatus*. Brown color formation starts to decrease at pH values of 8 and 9. Therefore, a pH of 7 serves as the optimal condition and is better



**Figure 1.** Visual observation of the AgNPs obtained by mycelia filtrate of *Aspergillus fumigatus* (a)  $\text{AgNO}_3$  (b) Mycelial filtrate of *A. fumigatus* before the addition of  $\text{AgNO}_3$  (1 mM) solution. (c) Color change reaction after exposure to  $\text{AgNO}_3$  solution for 24 h.

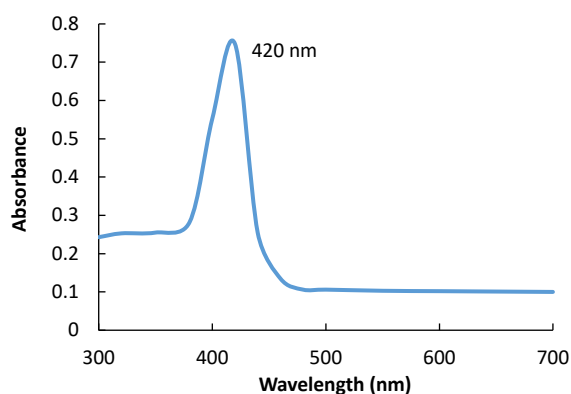


**Figure 2.** UV-vis spectrum analysis of biosynthesized AgNPs by *A. fumigatus* after 24 h of incubation.

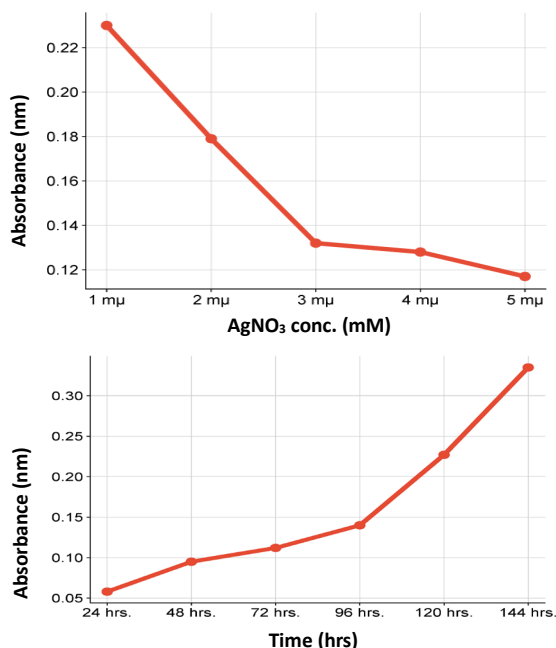


**Figure 3.** Effect of a) different concentrations of  $\text{AgNO}_3$  (mM); b) Effect of different incubation periods (hrs.) of the reaction mixture on the biogenesis of AgNPs by the mycelial filtrate of *A. fumigatus*.

for AgNPs production than alkaline or acidic media to produce AgNPs. These findings suggest that the biosynthesis of AgNPs is more favorable in a neutral environment than in an alkaline or acidic one, as shown in Figure 4b.

### Characterization Techniques of AgNPs

#### UV-Visible Spectroscopy

The formed AgNPs from *A. fumigatus* presented significant absorption bands at wavelengths of 400 nm and 420 nm. The maximum absorbance of the formed AgNPs was recorded at 420 nm (Figure 2).

#### Scanning Electron Microscopy (SEM)

The AgNPs' shape and size were investigated via SEM analysis, which revealed that the synthesized AgNPs have a spherical shape, are rough and that few particles are agglomerated. Agglomeration, a typical occurrence in AgNPs, is noted as a mechanism for achieving stability. AgNPs are a variation in particle size, and the average size was 56.91 nm as shown in Figure 5.

#### Elemental Diffraction X-Ray Spectroscopy (EDX)

Both the quantitative and qualitative statuses of the constituents that might be involved in the creation of AgNPs were determined via EDX analysis. The profile's modest oxygen peak and large silver signal suggested that silver ions had been reduced to elemental silver, possibly because of the biomolecules bonded to the AgNPs surface. No peaks connected to silver compounds were found. As illustrated in Figure 6, silver compounds are completely reduced to AgNPs. The presence of AgNPs in this study was validated by the significant Ag signal in the EDX spectra at 3 keV. As shown in Figure 6, the analysis of the elements showed that the sample included a significant amount of silver, with a weight percentage of 37.94%.

#### Fourier Transmission Infrared Spectroscopy (FTIR)

The biological components of the mycelial filtrate of *A. fumigatus* interacted with the nanoparticles presented peaks at 3433.06, 2915.58, 1631.72, and 1025.56  $\text{cm}^{-1}$  (Figure 7). The results indicated the presence of an amine group, as evidenced by a large and robust peak at 3433.06  $\text{cm}^{-1}$ , which corresponds to the stretching (N-H) functional group. However, the signal at 2915.58  $\text{cm}^{-1}$  indicated that silver ions connected to the OH group. Additionally, notable peaks were identified at 1631.72  $\text{cm}^{-1}$ , corresponding to (C=C) stretching in unsaturated ketones, which verified that the AgNPs included alkene groups. Additionally, another signal at 1025.56  $\text{cm}^{-1}$  indicated



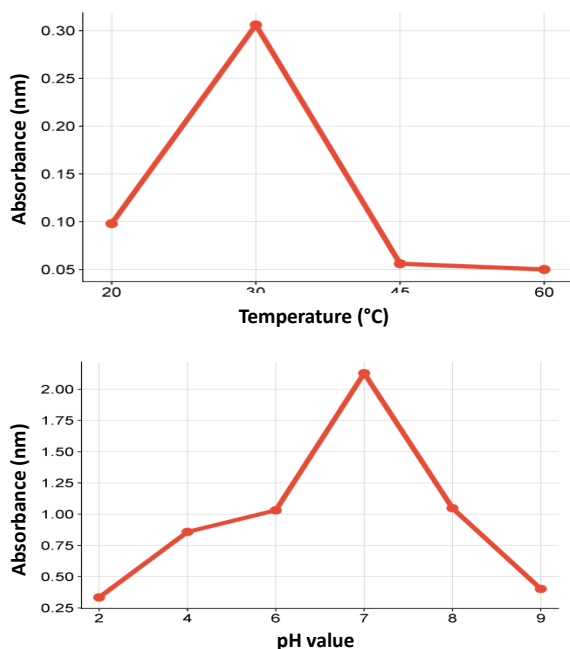


**Figure 4.** Biogenesis of AgNPs by the mycelial filtrate of *A. fumigatus* at a) different temperatures of the reaction mixture; b) different pH values

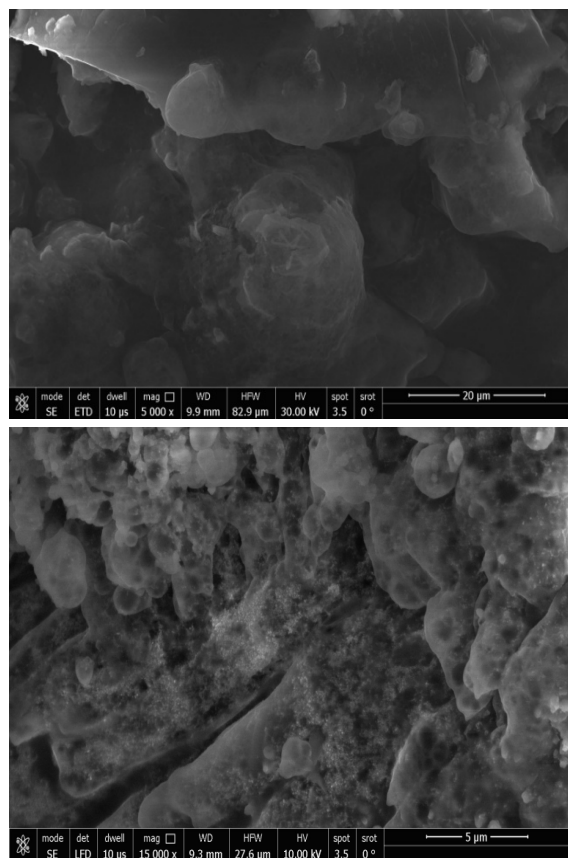


**Figure 5.** SEM micrographs of AgNPs created by *A. fumigatus* at various magnification: (a) SEM micrograph (5000X); (b) SEM micrograph (15000X).

that the (C-N) functional group was present, confirming the presence of aliphatic amines that are found in proteins and play a role in metal ion reduction. Finally, a peak was observed at  $622.3 \text{ cm}^{-1}$  for Ag which confirms the AgNPs formation.

### X-Ray Diffraction (XRD) Spectroscopy

XRD analysis was used to determine the AgNPs' structural information, and the particles were verified to be silver. The data in Table 1 and Figure 8 show four distinct peak patterns at  $2\theta$  values of  $20.733^\circ$ ,  $28.469^\circ$ ,  $32.253^\circ$ , and  $46.184^\circ$  for the AgNPs. The strong XRD patterns at  $2\theta = 20.733^\circ$  and  $28.469^\circ$  indicate the production of AgNPs with favorable crystal quality. The strong XRD peak at  $2\theta = 20.733^\circ$  is more intense than those of the other patterns. The size of the nanoparticles was calculated via Scherer's equation, and the AgNPs' average crystallite size was 56.91 nm.

### Antibacterial Activity Studies

The antibacterial properties of AgNPs produced by *A. fumigatus* were investigated against four tested pathogenic bacteria via the agar well diffusion technique, as illustrated in Table 2 and Figure 9. These results indicated that the mean inhibition zone against *Enterobacter cloacae* ATCC13047 was  $59 \pm 1.01$  mm, which was significantly greater than the mean inhibition zones observed for *Salmonella typhi* (ATCC7251), *Escherichia coli* (ATCC 25922) and *Proteus mirabilis* (ATCC 29906), which were  $54 \pm 1.15$ ,  $50 \pm 0.58$  and  $45 \pm 1.15$  mm, respectively, for each respective species, comparing these results with the results of positive and negative controls as shown in Figure 9.

### DISCUSSION

The biosynthesis of silver nanoparticles through green or biogenic methods provides a clean, environmentally friendly, and efficient approach to nanoparticle synthesis (Khleifat et al., 2022a). In this study, the capability of the endophytic fungus *A. fumigatus* to synthesize AgNPs, was evidenced by a color change to brown compared with that of the control sample. (Rai et al., 2021) reported that the fungal system is a versatile system that can produce metal nanoparticles outside of cells. (Momenah et al., 2023) revealed the same finding, confirming the biosynthesis of AgNPs from *A. fumigatus*, which visually displays the reduction of  $\text{Ag}^+$  to  $\text{Ag}^0$  by color changes. Research on the biosynthesis of AgNPs has revealed a change in color to brown in aqueous solution (Dhaka et al., 2023).

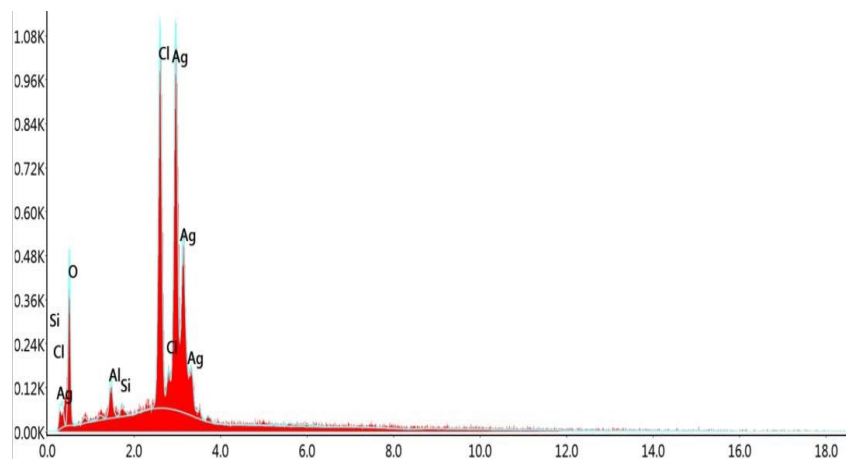


Figure 6. EDX spectrum of the biosynthesized AgNPs obtained from *A. fumigatus*.

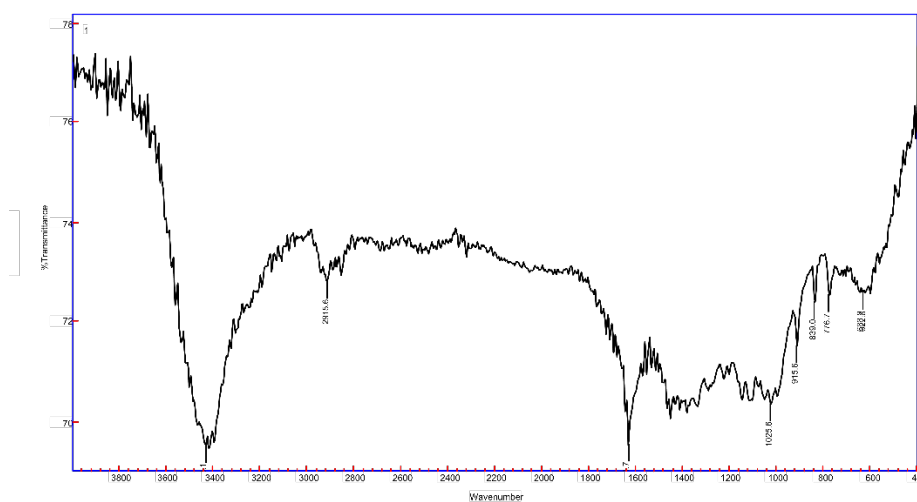


Figure 7. FTIR spectrum of the biosynthesized AgNPs obtained from *A. fumigatus*.

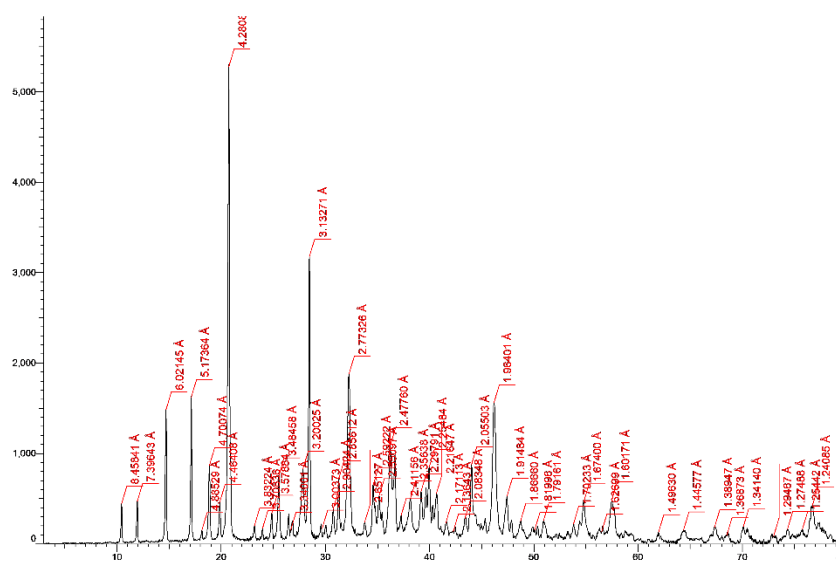
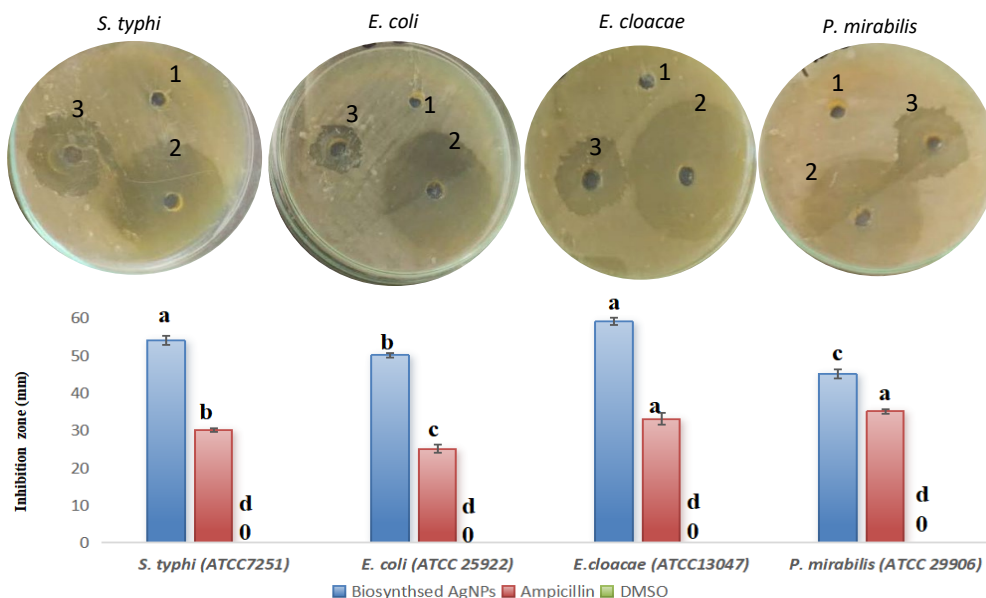


Figure 8. XRD diffractogram of the biosynthesized AgNPs.



**Figure 9.** *In vitro* antibacterial activities of the biosynthesized AgNPs. The numbers on the Petri dishes represent the following: 1 for 10% DMSO (negative control), 2 for biosynthesized AgNPs, and 3 for 1 mg/mL ampicillin (positive control). The small letters on the column chart indicate significant differences at  $P \leq 0.05$ .

The AgNPs were first characterized by using UV-visible spectroscopy. In this study, the maximum absorbance of the AgNPs was recorded at 420 nm. Similar findings revealed that the maximum wavelength of AgNPs was 420 nm (Gupta et al., 2022; EL-Zawawy et al., 2023). Furthermore, additional research reported a strong resonance peak located between 425 nm and 450 nm (Momenah et al., 2023; Ahmad et al., 2024). It is commonly recognized that any changes in these reaction parameters, including the metal ion concentration, metallic salt/reducing agent ratio, duration, temperature, and pH, alter the size, shape, synthesis, morphology and yield of metal nanoparticles (Guleria et al., 2022). Optimizing the unique properties and synthesis conditions of fungus-produced AgNPs is crucial (Rami et al., 2024).

The impact of the  $\text{AgNO}_3$  concentration on the optimal synthesis of silver nanoparticles was detected by increasing concentrations of silver salt (1 mM–5 mM) with a fixed amount of mycelia filtrate of *A. fumigatus* at a 1:1 ratio (v/v). In the present study, 1.0 mM  $\text{AgNO}_3$  was the most effective to produce AgNPs. The presence of excessive silver ions in the reaction media can lead to the creation of large nanoparticles with irregular shapes due to competition with functional groups from the fungal filtrate (Shahzad et al., 2019). These results: (1) revealed that the most stable AgNPs was synthesized with 1 mM  $\text{AgNO}_3$ , which prevented long-term aggregation; (2) agreed with those of (Osorio-Echavarría et al., 2021), who

found that the most efficient concentration for fungal AgNPs synthesis is often 1 mM  $\text{AgNO}_3$ ; (3) were in agreement with the data reported by (Lotfy et al., 2021) on the extracellular synthesis of AgNPs by *A. terreus*. In contrast, (Abdelmoneim et al., 2022) reported that an  $\text{AgNO}_3$  concentration of 6.0 mM was the most effective to produce AgNPs; and (4) agreed with other research showing that the yield of monodispersed AgNPs is significantly influenced by the concentration of  $\text{AgNO}_3$ . At low concentrations, it produces the best results, while at relatively high concentrations; it does not stabilize (Habibullah et al., 2022).

The incubation time serves as a crucial parameter for regulating reaction conditions and modifying the size and shape of nanoparticles (Javed et al., 2020). Time is a significant factor affecting AgNPs production, and varying incubation periods facilitate the determination of the optimum absorbance, which is correlated with the largest concentration of biosynthetic silver nanoparticles (Miu & Dinischiotu, 2022). In this study, AgNPs synthesis was investigated over a range of 24–144 hrs., revealing that the absorbance peak was achieved at 24 hrs. and continued to rise until 144 hrs. These results revealed that the fifth day was the optimal time for AgNPs production. Similarly, (El-Zawawy et al., 2023) reported that the fifth day was considered the optimum period for AgNP formation from *A. favipes*. In contrast, (Abdelmoneim et al., 2022) reported that



the greatest yield of AgNPs was observed after two days of incubation. As such, the optimal reaction times for the maximal reduction of Ag<sup>+</sup> ions to Ag<sup>0</sup> ranged between 1 and 144 hrs. according to different literature reports (Osorio-Echavarría et al., 2021; Abdelmoneim et al., 2022).

Different pH values have a significant effect on the structure and size of nanoparticles because pH can alter a molecule's charge, which may affect its stabilizing and capping capabilities and the production of nanoparticles (Verma & Mehata, 2016). In this investigation, the optimal pH for AgNPs production was a neutral pH of 7. These results showed that a neutral medium was preferable to alkaline or acidic media for AgNPs production (EL-Zawawy et al., 2023). Additionally, studies investigating that the Neutral pH is optimal for improved stability and biological uses, according to synthesis process optimization (Habibullah et al., 2022). The protein structure was impacted, denatured, and rendered ineffective at low pH levels, which caused the nanoparticles to aggregate (Srivastava & Alam, 2020). The main positive effect of reaction pH aligns with the findings of previous research (Al-Soub et al., 2022; EL-Zawawy et al., 2023).

Temperature has a significant effect on the nucleation mechanism that takes place during the synthesis of AgNPs because it is one of the most crucial variables influencing the rate of reaction (Kazemi et al., 2023). The temperature used during the biosynthesis of AgNPs significantly impacts the rate of synthesis, as well as the stability and size of the resulting AgNPs (Parameswaran et al., 2021). According to these findings, an incubation temperature of 25°C resulted in greater production of AgNPs, and the rate of AgNPs production increased with an increasing reaction mixture temperature until the temperature reached 30°C, after which it decreased as the temperature rose due to the reduced activity of enzymes, which affected the rate of AgNPs production. These findings aligned with those of (EL-Zawawy et al., 2023), who revealed that the optimum temperature for the biosynthesis of AgNPs was 25°C and that temperatures below and above 30°C reduce the formation of AgNPs.

Characterization of the formed AgNPs from *A. fumigatus* was detected by utilizing various analytical methods such as UV–Visible Spectroscopy, EDX, XRD, SEM, and FTIR (Abdel-Kareem et al., 2021; El-Naggar et al., 2024). Micrographs from SEM measurements

indicated that the AgNPs exhibited a nearly spherical structure. In the present study, the AgNPs had a spherical shape and exhibited clustering, with some agglomeration. The formation of nanoparticle aggregates suggested that the produced AgNPs had become more stable were previously obtained by (Momenah et al., 2023).

In the present study, a strong signal at 3 keV was observed in the EDX spectrum in the silver region, which verified the formation of AgNPs and confirmed their crystalline nature. Weaker signals from the Na, Si, S, P, Cl, and Ca atoms are also detected because of the presence of mycelial molecules or molecular elements connected with the formed AgNPs (Jafar et al., 2023). Furthermore, the lack of an N signal from AgNO<sub>3</sub> implies that the mycelial filtrate of *A. fumigatus* successfully effectively reduced Ag<sup>+</sup> to Ag<sup>0</sup>. Additionally, the EDX spectrum showed a significant silver peak that accounted for 37.94% of the total. These findings agree with those of (El-Naggar et al., 2024), who reported that the EDX spectrum showed a significant silver peak that accounted for 34.35% of the weight of the sample. The FTIR spectrum of the AgNPs revealed the presence of phenolic and alcoholic compounds in addition to proteins, which may be connected to the stabilization of the AgNPs by biomolecules and the reduction of silver nitrate into AgNPs. According to earlier research, FTIR analysis demonstrated the dual role of biological molecules that reduce and stabilize AgNPs (Ahmad et al., 2024; El-Naggar et al., 2024). The crystalline nature of the biosynthetic nanoparticles was proved by X-ray crystallography. XRD is thought to be a useful technique for confirming that the AgNPs are crystalline (Lotfy et al., 2021). In this study, the XRD analysis of AgNPs formed by *A. fumigatus* verified their high crystal quality, which was consistent with other studies of biosynthesized AgNPs (Hayat et al., 2023).

In this investigation, the average crystal size of the AgNPs was determined by the Scherrer equation. These findings were almost the same as those of (EL-Zawawy et al., 2023), who used Scherrer's equation to calculate the average crystal size of AgNPs formed by *Aspergillus favipes* AUMC 15772 endophytic fungi. AgNPs possess remarkable antimicrobial properties that remain stable under extreme stress conditions, making them suitable for the management of several illnesses (Huq et al., 2022). In this investigation, AgNPs showed strong significant antibacterial efficacy against all tested pathogenic bacterial strains, including *Enterobacter*

*cloacae* (ATCC13047), *Salmonella typhi* (ATCC7251), *Escherichia coli* (ATCC 25922), and *Proteus mirabilis* (ATCC 29906). Previous research has highlighted the antibacterial effects of different AgNPs and their potential to effectively hinder the growth of several tested pathogenic bacteria, such as *Escherichia coli*, *Pseudomonas aeruginosa*, *Klebsiella pneumoniae*, *Enterobacter cloacae*, *Shigella* sp., *Staphylococcus aureus*, and *Staphylococcus epidermidis* (Al-Soub et al., 2022; Khleifat et al., 2022b; Husein et al., 2023). The unique surface-to-volume ratio of silver nanoparticles derived from fungal endophytes contributes to their exceptional antibacterial activity, even at low concentrations, against a diverse array of pathogenic bacterial strains (Gezaf et al., 2022).

## CONCLUSIONS

The field of nanotechnology has significantly expanded in recent years and has been widely applied in the realms of healthcare, industry, and the environment. This study demonstrated the ability of the endophytic fungus *A. fumigatus* to synthesize AgNPs, with a strong peak at 420 nm. The optimization of the mycosynthesis of AgNPs by different parameters, such as the AgNO<sub>3</sub> concentration, incubation time, pH, and temperature, revealed a significant positive effect on the formation of AgNPs. The properties of the AgNPs were characterized via UV–visible spectroscopy, SEM, EDX, XRD and FT-IR analyses. The shapes and size of the produced AgNPs were detected via SEM. FTIR examination revealed that the phenolic, carboxyl, and hydroxyl groups of the AgNPs were responsible for the reduction of silver, whereas the amide linkage amino acid was responsible for the stabilization of the AgNPs. Additionally, the XRD patterns revealed the naturally crystalline structure of the AgNPs. Under ideal conditions, endophytic *A. fumigatus* can create AgNPs and demonstrate significant antimicrobial activity against human pathogenic bacteria. The formed AgNPs enhance antibacterial activity, highlighting their potential in future research.

## ACKNOWLEDGMENTS

We express our sincere thanks and gratitude to the Botany Department, Faculty of Science, Aswan University, for supporting and providing the requirements of scientific research.

## AUTHORS' CONTRIBUTIONS

Doaa MAK contributed to the study design, material preparation, methodology, data collection and analysis; wrote the main manuscript text; and Noura

SHAH contributed to the data analysis, read and reviewed the final manuscript. All authors have read and agreed to the published version of the manuscript

## DATA AVAILABILITY

The data used and analyzed in this study are available from the corresponding author upon reasonable request.

## FUNDING

This research did not receive any external funding.

## CONFLICT OF INTEREST

The authors declare that there are no conflicts of interest.

## REFERENCES

- Abbas, R., Luo J., Qi X., Naz, A., Khan. IA., Liu, H., Yu, S., & Wei, J. (2024) Silver Nanoparticles: Synthesis, Structure, Properties and Applications. *Nanomaterials*, 14,1425. <https://doi.org/10.3390/nano14171425>.
- Abdel-Kareem, M.M., Zohri, A.A., & Rasmey, A.M. (2021) Biosynthesis of Silver Nanoparticles by *Aspergillus sakultaensis* and its Antibacterial Activity against Human Pathogens. *Egyptian Journal of Microbiology*, 56, 11-24. <https://doi.org/10.21608/ejm.2021.46387.1177>.
- Abdelmoneim, H.M., Taha, T.H., Elnouby, M.S., & AbuShady, H.M. (2022) Extracellular biosynthesis, OVAT/statistical optimization, and characterization of silver nanoparticles (AgNPs) using *Leclercia adecarboxylata* THHM and its antimicrobial activity. *Microbial Cell Factories*, 21(1), 277. <https://doi.org/10.1186/s12934-022-01998-9>.
- Ahmad, N., Malik, M.A., Wani, A-H., & Bhat, M.Y. (2024) Biogenic silver nanoparticles from fungal sources: Synthesis, characterization, and antifungal potential. *Microbial pathogenesis*, 193, 106742. <https://doi.org/10.1016/j.micpath.2024.106742>.
- Ali, M.H., Azad, M.A., Khan, K.A., Rahman M.O., Chakma, U., & Kumer, A. (2023) Analysis of Crystallographic Structures and Properties of Silver Nanoparticles Synthesized Using PKL Extract and Nanoscale Characterization Techniques. *American Chemical Society omega*, 8(31), 28133-28142. <https://doi.org/10.1021/acsomega.3c01261>.
- Al-Limoun, M., Qaralleh, H.N., Khleifat, K.M., Al-Anber, M., Al-Tarawneh, A., Al-sharafa, K., & Al-soub, T. (2020) Culture media composition and reduction potential optimization of mycelia-free filtrate for the biosynthesis of silver nanoparticles using the fungus *Tritirachium oryzae* W5H. *Current nanoscience*, 16(5),757–769. <https://doi.org/10.2174/1573413715666190725111956>.
- Al-Soub, A, Khleifat, K, Al-Tarawneh, A, Al-Limoun, M, Alfarrayeh, M, Al Sarayreh, A., Al Qaisi, Y., Qaralleh, H., Alqaraleh, M., & Albashaireh, A. (2022) Silver nanoparticles biosynthesis using an airborne fungal

- isolate, *Aspergillus flavus*: optimization, characterization and antibacterial activity. *Iranian Journal of Microbiology*, 14(4), 518-528. <https://doi.org/10.18502/ijm.v14i4.10238>.
- Baker, A., Iram, S., Syed, A., Elgorban, A.M., Bahkali, A.H., Ahmad, K., Khan, M.S., & Kim, J. (2021) Fruit derived potentially bioactive bioengineered silver nanoparticles. *International Journal of Nanomedicine*, 16, 7711-7726. <https://doi.org/10.2147/IJN.S330763>.
- Balakumaran, M., Ramachandran, R., Balashanmugam, P., Mukeshkumar, D., & Kalaichelvan, P. (2016) Mycosynthesis of silver and gold nanoparticles: optimization, characterization and antimicrobial activity against human pathogens. *Microbiological research*, 182, 8-20. <https://doi.org/10.1016/j.micres.2015.09.009>.
- Dadayya, M., Subhakar, A., Gurubasajar, N., Thippeswamy, M.G., Veeranna, S.H., & Basaiah, T. (2023) Green Synthesis of Silver Nanoparticles from Endophytic Fungus *Alternaria carthami*-KUMBMDBT-30. *Asian journal of biological sciences*, 12(1), 192-197. <https://doi.org/10.5530/ajbls.2023.12.26>.
- Dhaka, A., Mali, S.C., Sharma, S., & Trivedi, R. (2023) A review on biological synthesis of silver nanoparticles and their potential applications. *Results in Chemistry*, 6, 101108. <https://doi.org/10.1016/j.rechem.2023.101108>.
- Dubey, S.P., Lahtinen, M., & Sillanpaa, M. (2010) Tansy fruit mediated greener synthesis of silver and gold nanoparticles. *Process Biochemistry*, 45, 1065-1071. <http://dx.doi.org/10.1016/j.procbio.2010.03.024>.
- El-Khouly, N., Fergani, M., El-temsah, M., El-Saady, K., shahin, M. (2024). Impact of Integration between Soil Application of Phosphorus and Foliar Spraying of Nano Potassium, Iron and Boron on the Productivity and Quality of Peanuts.. *Egyptian Journal of Botany*, 64(3), 130-147. doi: 10.21608/ejbo.2024.213993.2356.
- El-Naggar, N.E.A., Shweqa, N.S., Abdelmigid, H.M., Alyamani, A.A., Elshafey, N., Soliman, H.M., & Heikal, Y.M. (2024) Myco-Biosynthesis of Silver Nanoparticles, Optimization, Characterization, and In Silico Anticancer Activities by Molecular Docking Approach against Hepatic and Breast Cancer. *Biomolecules*, 14(9), 1170. <https://doi.org/10.3390/biom14091170>.
- EL-Zawawy, N.A., Abou-Zeid, A.M., Beltagy, D.M., Hantera, N.H., & Nough, H.S. (2023) Mycosynthesis of silver nanoparticles from endophytic *Aspergillus favipes* AUMC 15772: ovat-statistical optimization, characterization and biological activities. *Microbial Cell Factories*, 22, 228. <https://doi.org/10.1186/s12934-023-02238-4>.
- Fadiji, A.E., Mortimer, P.E., Xu, J., Ebenso, E.E., & Babalola, O.O. (2022) Biosynthesis of Nanoparticles Using Endophytes: A Novel Approach for Enhancing Plant Growth and Sustainable Agriculture. *Sustainability*, 14, 10839. <https://doi.org/10.3390/su141710839>.
- Farrag, H.M.M., Mostafa, F.A.M., Mohamed, M.E., & Huseein, E.A.M. (2020) Green biosynthesis of silver nanoparticles by *Aspergillus niger* and its antiamoebic effect against *Allovahlkampfia spelaea* trophozoite and cyst. *Experimental parasitology*, 219, 108031. <https://doi.org/10.1016/j.exppara.2020.108031>.
- Gezaf, S.A., Hamedo, H.A., Ibrahim, A.A., & Mossa, M.I. (2022) Mycosynthesis of silver nanoparticles by endophytic Fungi: Mechanism, characterization techniques and their applications. *Microbial Biosystems*, 7(2), 48-65. <https://doi.org/10.21608/MB.2023.185718.1066>.
- Guleria, G., Thakur, S., Shandilya, M., Sharma, S., Thakur, S., & Kalia, S. (2022) Nanotechnology for sustainable agro-food systems: the need and role of nanoparticles in protecting plants and improving crop productivity. *Plant Physiology and Biochemistry*, 194, 533-549. <https://doi.org/10.1016/j.plaphy.2022.12.004>.
- Gupta, P., Rai, N., Verma, A., Saikia, D., Singh, S.P., Kumar, R., Singh, S.K., Kumar, D., & Gautam, V. (2022) Green-Based Approach to Synthesize Silver Nanoparticles Using the Fungal Endophyte *Penicillium oxalicum* and Their Antimicrobial, Antioxidant, and In Vitro Anticancer Potential. *American Chemical Society omega*, 7(50), 46653-46673. <https://doi.org/10.1021/acsomega.2c05605>.
- Habibullah, G., Viktorova, J., Ulbrich, P., & Ruml, R. (2022) Effect of the physicochemical changes in the antimicrobial durability of green synthesized silver nanoparticles during their long-term storage. *RSC Advances*, 12(47), 30386-30403. <https://doi.org/10.1039/d2ra04667a>.
- Hayat, F., Khanum, F., Li, J., Iqbal, S., Khan, U., Javed, H.U., Razzaq, M.K., Altaf, M.A., Peng, Y., Ma, X., Li, C., Tu, P., & Chen, J. (2023) Nanoparticles and their potential role in plant adaptation to abiotic stress in horticultural crops: A review. *Scientia Horticulturae*, 321(1), 112285. <https://doi.org/10.1016/j.scienta.2023.112285>.
- Huq, A. (2020) Green synthesis of silver nanoparticles using *Pseudoduganella eburnea* MAHUQ-39 and their antimicrobial mechanisms investigation against drug resistant human pathogens. *International Journal of Molecular Sciences*, 21 (4), 1510. <https://doi.org/10.3390/ijms21041510>.
- Huq, Md A., & Akter, S. (2021) Bacterial mediated rapid and facile synthesis of silver nanoparticles and their antimicrobial efficacy against pathogenic microorganisms. *Materials*, 14(10), 2615. <https://doi.org/10.3390/ma14102615>.
- Huq, Md A., Ashrafudoulla, M., Rahman, S.R., Balusamy, M.M., & Akter, S. (2022) Green synthesis and potential antibacterial applications of bioactive silver nanoparticles: a review. *Polymers*, 14(4), 742. <https://doi.org/10.3390/polym14040742>.
- Husein, N.F., Al-Tarawneh, A.A., Al-Rawashdeh, S.R., Khleifat., K., Al-Limoun, M., Alfarrayeh, I., Awwad, A.E., AlSarayreh, A.Z., & Al-Qaisi, Y. (2023) *Ruta graveolens* methanol extract, fungal-mediated biosynthesized silver nanoparticles, and their combinations inhibit

- pathogenic bacteria. *Journal of Advanced Pharmacy Education and Research*, 13 (2), 43-52. <https://doi.org/10.51847/h8sagkiapx>.
- Isaq, M., Ramachandra, Y.L., Rai, P., Chavan, A., Sekar, R., Lee, M-J., & Somu, P. (2023) Biogenic synthesized silver nanoparticles using fungal endophyte *Cladosporium oxysporum* of *Vateria indica* induce apoptosis in human colon cancer cell line via elevated intracellular ROS generation and cell cycle arrest. *Journal of molecular liquids*, 386 (15), 122601. <https://doi.org/10.1016/j.molliq.2023.122601>.
- Jafar, S.S., Saallah, S., Misson, M., Siddiquee, S., Roslan, J., & Lenggono, W. (2023) Green synthesis of fower-like carrageenan-silver nanoparticles and elucidation of its physicochemical and antibacterial properties. *Molecules*, 28(2), 907. <https://doi.org/10.3390/molecules28020907>.
- Janakiraman, V., Govindarajan, K., & Magesh, C.R. (2019) Biosynthesis of Silver Nanoparticles from Endophytic Fungi, and its Cytotoxic Activity. *BioNanoScience*, 9, 573-579. <https://doi.org/10.1007/s12668-019-00631-1>.
- Javed, B., Nadhman, A., & Mashwani, Z.R. (2020) Optimization, characterization and antimicrobial activity of silver nanoparticles against plant bacterial pathogens phyto-synthesized by *Mentha longifolia*. *Materials research express*, 7(8), 085406. <https://doi.org/10.1088/2053-1591/abaf19>.
- Kazemi, S., Hosseingholian, A., Gohari, S.D., Feirahi, F., Moammeri, F., Mesbahian, G., Moghaddam, Z.S., & Ren, Q. (2023) Recent advances in green synthesized nanoparticles: from production to application. *Materials Today Sustainability*, 24, 100500. <https://doi.org/10.1016/j.mtsust.2023.100500>.
- Keshari, A.K., Srivastava, R., Singh, P., Yadav, V.B., & Nath, G. (2020) Antioxidant and antibacterial activity of silver nanoparticles synthesized by *Cestrum nocturnum*. *Journal of Ayurveda and Integrative Medicine*, 11(1):37-44. <https://doi.org/10.1016/j.jaim.2017.11.003>.
- Khleifat, K., Alqaraleh, M., Al-Limoun, M., Alfarayeh, I., Khatib, R., Qaralleh, H., & Hajleh, M.A. (2022a) The ability of *Rhizopus stolonifer* MR11 to biosynthesize silver nanoparticles in response to various culture media components and optimization of process parameters required at each stage of biosynthesis. *Journal of Ecological Engineering*, 23(8), 2022. <https://doi.org/10.12911/22998993/150673>.
- Khleifat, K., Qaralleh, H., Al-Limoun, M., Alqaraleh, M., Abu Hajleh, M.N., Al-Frouhk, R., Al-Omari, L., Al Buqain, R., & Dmour, S.M. (2022b) Antibacterial activity of silver nanoparticles synthesized by *Aspergillus flavus* and its synergistic effect with antibiotics. *Journal of Pure and Applied Microbiology*, 16 (3), 1722-1735. <https://doi.org/10.22207/JPAM.16.3.13>.
- Lotfy, W.A., Alkersh, B.M., Sabry, S.A., & Ghazlan, H.A. (2021) Biosynthesis of Silver Nanoparticles by *Aspergillus terreus*: Characterization, Optimization, and Biological Activities. *Frontiers in Bioengineering and Biotechnology*, 9, 633468. <https://doi.org/10.3389/fbioe.2021.633468>.
- Miu, B.A., & Dinischiotu, A. (2022) New Green Approaches in Nanoparticles Synthesis: An Overview. *Molecules*, 27(19), 6472. <https://doi.org/10.3390/molecules27196472>.
- Momenah, A.M., Hariri, S.H., Abdel-razik, N.E., Bantun, F., Khan, S., Alghamdi, S., & Tasleem, S. (2023) *Aspergillus Fumigatus*-Mediated Biosynthesis of Silver Nanoparticles Efficiency, Characterization, and Antibacterial Activity Against Different Human Pathogens. *Egyptian Academic Journal of Biological Sciences*, 15(1), 353-364. <https://doi.org/10.21608/EAJBSC.2023.294953>.
- Moradi, N., Sadravi, M., Hajati, S., & Hamzehzarghani, H. (2024) Biosynthesized silver nanoparticles using *Trichoderma harzianum* reduce charcoal rot disease in bean. *Rhizosphere*, 29, 100828. <https://doi.org/10.1016/j.rhisph.2023.100828>.
- Osorio-Echavarría, J., Ossa-Orozco, C.P., & Gómez-Vanegas, N.A. (2021) Synthesis of silver nanoparticles using white-rot fungus *Anamorphous Bjerkandera* sp. R1: influence of silver nitrate concentration and fungus growth time. *Scientific reports*, 15(11):3842. <https://doi.org/10.1038/s41598-021-82514-8>.
- Parameswaran, S., Karthickeyan, D., & Venugopal, T. (2021) Effect of temperature on green synthesized silver nanoparticles using water and methanol. *Materials Today Proceedings*, 45, 5506-5510. <https://doi.org/10.1016/j.matpr.2021.02.232>.
- Paramo, L.A., Feregrino-Pérez, A.A., Guevara, R., Mendoza, S., & Esquivel, K. (2020) Nanoparticles in agroindustry: Applications, toxicity, challenges, and trends. *Nanomaterials*, 10(9), 1654. <https://doi.org/10.3390/nano10091654>.
- Rai, M., Bonde, S., Golinska, P., Trzcinska-Wencel, J., Gade, A., Abd-Elsalam, K.A., Shende, S., Gaikwad S., & Ingle, A.P. (2021) *Fusarium* as a Novel Fungus for the Synthesis of Nanoparticles: Mechanism and Applications. *Journal of Fungi*, 7, 139. <https://doi.org/10.3390/jof7020139>.
- Rami, M.R., Meskini, M., & Sharafabad, B.E. (2024) Fungal-mediated nanoparticles for industrial applications: synthesis and mechanism of action. *Journal of Infection and Public Health*, 17(10), 102536. <https://doi.org/10.1016/j.jiph.2024.102536>.
- Ramos, M.M., Morais, E.D.S., Sena, I.D.S., Lima, A.L., De Oliveira, F.R., De Freitas, C.M., Fernandes, C.P., De Carvalho, J.C.T., & Ferreira, I.M. (2020) Silver nanoparticle from whole cells of the fungi *Trichoderma* spp. isolated from Brazilian Amazon. *Biotechnology letters*, 42(5), 833-843. <https://doi.org/10.1007/s10529-020-02819-y>.
- Rodríguez-Serrano, C., Guzmán-Moreno, J., Ángeles-Chávez, C., Rodríguez-González, V., Ortega-Sigala, J.J., Ramírez-Santoyo, R.M., Vidales-Rodríguez, L.E. (2020) Biosynthesis of silver nanoparticles by *Fusarium scirpi* and its potential as antimicrobial agent against uropathogenic *Escherichia coli* biofilms. *PLoS ONE*,

- 15(3), e0230275. <https://doi.org/10.1371/journal.pone.0230275>. eCollection 2020.
- Shahzad, A., Saeed, H., Iqtedar, M., Hussain, S.Z., Kaleem, A., Abdullah, R., & Chaudhary, A. (2019) Size-controlled production of silver nanoparticles by *Aspergillus fumigatus* BTCB10: likely antibacterial and cytotoxic effects. *Journal of nanomaterials*, 1-14. <https://doi.org/10.1155/2019/5168698>.
- Soliman, A., Shahin, S., Goda, S. (2024). Incorporation of Nanotechnology in Propagation Treatments by Cuttings of Jojoba (*Simmondsia chinensis* (Link) Schneider) Shrubs in Egypt and South Africa. *Egyptian Journal of Botany*, 64(1), 65-86. doi: 10.21608/ejbo.2023.198552.2273
- Srivastava, R., & Alam, M.S. (2020) Influence of micelles on protein's denaturation. *Journal of Biological Macromolecules*, 145(15), 252-261. <https://doi.org/10.1016/j.ijbiomac.2019.12.154>.
- Verma, A., & Mehata, M.S. (2016) Controllable synthesis of silver nanoparticles using neem leaves and their antimicrobial activity. *Journal of Radiation Research and Applied Sciences*, 9(1), 109-15. <https://doi.org/10.1016/j.jrras.2015.11.001>.
- Xue, B., He, D., Gao, S., Wang, D., Yokoyama, K., & Wang, L. (2016) Biosynthesis of silver nanoparticles by the fungus *Arthroderma fulvum* and its antifungal activity against genera of *Candida*, *Aspergillus* and *Fusarium*. *International Journal of Nanomedicine*, 11, 1899-1906. <https://doi.org/10.2147/IJN.S98339>. eCollection 2016.
- Yassin, MA, Elgorban, A.M., El-Samawaty, A.M.A., & Almunqedhi, B.M.A. (2021) Biosynthesis of silver nanoparticles using *Penicillium verrucosum* and analysis of their antifungal activity. *Journal of biological sciences*, 28(4), 2123-2127. <https://doi.org/10.1016/j.sjbs.2021.01.063>.